LA-UR-08- 5056

Approved for public release;
distribution is unlimited.

Title:	Probing the Chemistry, Electronic Structure and Redox Energetics in Pentavalent Organometallic Actinide Complexes
Author(s):	C.R. Graves, A.E. Vaughn, D.E. Morris, J.L. Kiplinger
Intended for:	Inorganic Chemistry

Los Alamos
NATIONAL LABORATORY
EST.1943

Form 836 (7/06)

ketimide complex $(C_5Me_5)_2U(=N\text{-}2,6\text{-}^iPr_2\text{-}C_6H_3)(N=CPh_2)$ (**18**). The complexes have been isolated in good yield and characterized using various combinations of ^1H NMR spectroscopy, elemental analysis, mass spectrometry, single crystal X-ray diffraction, cyclic voltammetry, UV-visible-NIR absorption spectroscopy, and magnetic susceptibility measurements. All $(C_5Me_5)_2U(=N\text{-}Ar)(Y)$ complexes exhibit U^V/U^{IV} and U^{VI}/U^V redox couples by voltammetry, with the potential separation between these metal-based couples remaining essentially constant at ~1.50 V.

Introduction

Complexes of the early actinides (Th-Pu) have gained considerable prominence in organometallic chemistry as they have been shown to undergo chemistries not observed with their transition- or lanthanide metal counterparts.[1-9] Further, while bonding in f-element complexes has historically been considered to be ionic, the issue of covalency remains a subject of debate in the area of actinide science,[10-12] and studies aimed at elucidating key bonding interactions with 5f-orbitals continue to garner attention. Towards this end, our interests have focused on the role that metal oxidation state plays in the structure, reactivity and spectral properties of organouranium complexes. In recent years, tetravalent and hexavalent complexes have dominated the landscape of uranium chemistry,[13,14] with the corresponding pentavalent systems remaining rare. This is presumably a consequence of their instability towards redistribution,[15,16] and most of our current knowledge of the physicochemical properties of uranium in this oxidation state come from classical coordination complexes of the halides, (e.g., UX_5 where X = halide).[17,18]

From a heuristic perspective, the U^V oxidation state with its simple $5f^1$ valence electronic configuration remains a highly attractive target. While more structurally elaborate uranium(V) systems have been noted in the literature, specifically those containing metal–nitrogen and –oxygen bonds,[19] organometallic systems are comparatively less common.[13,20] Importantly, the synthetic routes available for accessing pentavalent systems have been limited, relying on either the one-electron oxidation of U^{IV} complexes with silver[20a,21] or thallium[22] salts to give cationic U^V species, or by reacting trivalent uranium complexes with powerful two-electron oxidants such as azides or *N*-oxides to give the corresponding U^V-imido or -oxo complexes, respectively.[19b,23-26] While successful, these routes utilize reagents that can be difficult to handle and control,[27] and are also synthetically limited in scope and cannot be easily fine-tuned.

We recently reported[28,29] a general and versatile Cu(I)-based oxidation procedure that enables easy access to pentavalent organometallic uranium complexes of the type $(C_5Me_5)_2U(=N\text{-}Ar)(X)$ (where X = halogen) from the corresponding U^{IV}-imido systems $((C_5Me_5)_2U(=N\text{-}2,4,6\text{-}{}^tBu_3\text{-}C_6H_2)$ (**1**);[30]

$(C_5Me_5)_2U(=N\text{-}2,6\text{-}^iPr_2\text{-}C_6H_3)$ (**2**[23]) (eq 1). While the one-electron oxidations utilizing silver salts result in cationic uranium complexes, this Cu-based oxidative functionalization results in neutral U^V species which feature a bent-metallocene framework with the imido and halide ligands contained within the metallocene wedge.

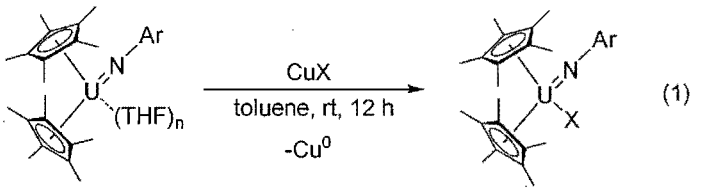

(1)

1: Ar = 2,4,6-^{t}Bu$_3$-C$_6$H$_2$, n = 0

2: Ar = 2,6-^{i}Pr$_2$-C$_6$H$_3$, n = 1

3: Ar = 2,4,6-^{t}Bu$_3$-C$_6$H$_2$, X = F
4: Ar = 2,4,6-^{t}Bu$_3$-C$_6$H$_2$, X = Cl
5: Ar = 2,4,6-^{t}Bu$_3$-C$_6$H$_2$, X = Br
6: Ar = 2,4,6-^{t}Bu$_3$-C$_6$H$_2$, X = I

7: Ar = 2,6-^{i}Pr$_2$-C$_6$H$_3$, X = F
8: Ar = 2,6-^{i}Pr$_2$-C$_6$H$_3$, X = Cl
9: Ar = 2,6-^{i}Pr$_2$-C$_6$H$_3$, X = Br
10: Ar = 2,6-^{i}Pr$_2$-C$_6$H$_3$, X = I

Applicable for the synthesis of the full suite of halides (X = F, Cl, Br, I), this protocol allowed for a systematic study of the electronic structure and bonding of pentavalent uranium chemistry — a study which suggested that minor differences existed between the structures as the halide ligand was varied. As such, our search has been broadened to the synthesis of non-halogenated U^V-imido complexes, $(C_5Me_5)_2U(=N\text{-}Ar)(Y)$, where Y represents a non-halide anionic ligand, in order to investigate larger perturbations in the bonding environment around the uranium metal. Herein, we report our progress in the synthesis of substituted U^V-imido complexes using various routes: (1) Direct oxidation of U^{IV}-imido complexes with copper(I) salts; (2) Salt metathesis with U^V-imido halides; (3) Protonolysis and insertion of an U^V-imido alkyl or aryl complex with H-N=CPh$_2$ or N≡C-Ph, respectively, to form a U^V-imido ketimide complex. Further, we report and compare the crystallographic, electrochemical, spectroscopic and magnetic characterization of the pentavalent uranium $(C_5Me_5)_2U(=N\text{-}Ar)(Y)$ series (Y = OTf, SPh, C≡C-Ph, NPh$_2$, OPh, N=CPh$_2$) to further interrogate the molecular, electronic, and magnetic structures of this new class of uranium complexes.

Results and Discussion

Synthesis and Structural Characterization.

A - Direct Oxidation

The direct oxidation of complex **2** with functionalized copper(I) salts was examined as a primary route for the synthesis of $(C_5Me_5)_2U(=N\text{-}2,6\text{-}^iPr_2\text{-}C_6H_3)(Y)$ complexes with extended ligand sets (Y ≠ halogen). A logical extension of the halide chemistry, reaction of **2** with one equivalent of the $(CuOTf)_2$·toluene adduct (OTf = OSO_2CF_3) afforded the U^V-imido triflate derivative, $(C_5Me_5)_2U(=N\text{-}2,6\text{-}^iPr_2\text{-}C_6H_3)(OTf)$ (**11**), in good isolated yield (eq 2).[28] The corresponding oxidation utilizing the copper halides were optimized to occur over 12 h using an excess of the oxidant (5 equiv); however use of excess $(CuOTf)_2$·toluene or extended reaction times lead to dramatic decomposition of the triflate product. Conversely, $(C_5Me_5)_2U(=N\text{-}2,6\text{-}^iPr_2\text{-}C_6H_3)(SPh)$ (**12**)[28] and $(C_5Me_5)_2U(=N\text{-}2,6\text{-}^iPr_2\text{-}C_6H_3)(C{\equiv}C\text{-}Ph)$ (**13**)[31] could only be prepared by reacting **2** with excess oxidant (CuSPh or CuC≡C-Ph, 5 equiv) at 75 °C over 12 h. Following workup, complexes **11-13** were reproducibly isolated as analytically pure solids and were characterized by a combination of ^1H NMR, electrochemistry, UV-visible near-IR spectroscopy, elemental and mass spectrometric analyses, and magnetic susceptibility.

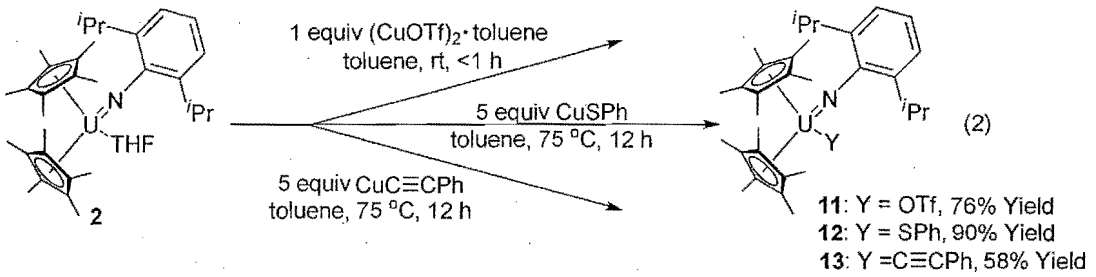

The identities of compounds **11** and **12** were confirmed by single-crystal X-ray crystallography.[28] Like their halide counterparts, these bent-metallocene complexes contain the imido and Y ligands contained within the metallocene wedge. A list of selected geometric parameters can be found in Table 1. Both **11** and **12** have nearly linear $U{=}N\text{-}C_{Ar}$ angles (168.3(5)° and 171.6(3)°, respectively) and short $U{=}N_{imido}$ bond distances (1.9575(5) Å and 1.976(4) Å, respectively), which compare well with the corresponding metrical parameters observed for the U^V-imido halides (**3**, **5**, **8-10**)[29] and other high-valent uranium (U^{IV}-U^{VI}) imido compounds.[32] To the best of our knowledge, **11** is the first structurally

characterized pentavalent uranium species incorporating a triflate group. At 2.378(4) Å the U-OTf bond length observed in **11** compares well with those reported for other structurally characterized uranium triflate complexes. For example, $(C_5Me_5)_2U[\eta^2\text{-}(N,N')\text{-}CH_3\text{-}N\text{-}N{=}CPh_2](OTf)$ has a U-OTf bond distance of 2.395 Å,[33] while the U^{IV} bis(triflate) complexes $(C_5Me_5)_2U(OTf)_2{\cdot}OH_2$ and $(C_5H_5)_2U(OTf)_2(pyridine)_2$ have U-OTf bond lengths of 2.36(1) Å and 2.40(1) Å[34] and 2.395(4) Å and 2.385(4) Å,[35] respectively. With regard to **12**, one other pentavalent organouranium complex with a U-S bond has been reported: $[Na(18\text{-crown-}6)(THF)][(\eta^8\text{-}C_8H_8)U(C_4H_4S_4)_2]$, with U-S bond lengths in the range 2.68-2.70 Å.[36,37] Not surprisingly, the U-S distance of 2.7230(13) Å found for neutral **12** is slightly longer than the range observed for the U^V cationic system. It is in agreement with U-S bond distances observed for complexes of uranium in other oxidation states.[38]

Table 1. Selected Metrical Parameters for the $(C_5Me_5)_2U(=N\text{-}2,6\text{-}^iPr_2\text{-}C_6H_3)(Y)$ Complexes **8-12, 14, 18.**

	$C_5Me_{5(cent)}$-M	$C_5Me_{5(cent)}$-M-$C_5Me_{5(cent)}$	Imido Parameters			X/Y Ligand Parameters		N-U-X/Y (°)
			U-N (Å)	N-C (Å)	U-N-C (°)			
8 X = Cl	2.505, 2.453	134.87	1.963(4)	1.404(7)	169.6(4)	**U-Cl (Å)** 2.6209(15)		**N-U-Cl** 105.79(13)
9 X = Br	2.523, 2.452	137.98	1.969(7)	1.40(2)	172.2(9)	**U-Br (Å)** 2.789(3)		**N-U-Br** 105.3(2)
10 X = I	2.454, 2.459	134.07	1.974(7)	1.406(10)	170.7(6)	**U-I (Å)** 3.0385(7)		**N-U-I** 106.6(2)
11 Y = OTf	2.435, 2.440	135.92	1.9575(5)	1.416(8)	168.3(5)	**U-O (Å)** 2.378	**U-O-S (°)** 160.4(3)	**N-U-O** 109.16(19)
12 Y = SPh	2.466, 2.457	136.24	1.976(4)	1.398(6)	171.6(3)	**U-S (Å)** 2.7230(13)	**U-S-C(°)** 131.08(17)	**N-U-S** 103.35(12)
14 Y = NPh_2	2.511, 2.530	125.01	1.984(4)	1.399(6)	174.0(3)	**U-N (Å)** 2.322(4)		**N-U-N** 93.73(15)
18 Y = N=CPh_2	2.493, 2.484	138.32	2.012(4)	1.391(7)	174.6(4)	**U-N (Å)** 2.199(4)	**U-N-C (°)** 177.8(4)	**N-U-N** 111.99(17)

B - Salt Metathesis

An alternative route for the generation of substituted of U^V-imido complexes is salt metathesis between the imido iodide $(C_5Me_5)_2U(=N\text{-}2,6\text{-}^iPr_2\text{-}C_6H_3)(I)$ (**10**)[39] and selected alkali metal reagents. This pathway is particularly attractive for those situations where the copper reagent [Cu(I)L] required for the direct oxidation pathway outlined above is unavailable or unstable, thereby dramatically expanding the synthetic utility of the U^V-imido chemistry. As illustrated in Scheme 1, $(C_5Me_5)_2U(=N\text{-}2,6\text{-}^iPr_2\text{-}C_6H_3)(NPh_2)$ (**14**) was prepared by the reaction between **10** and $KNPh_2$. While this reaction occurred at room temperature over 12 h, the corresponding synthesis for $(C_5Me_5)_2U(=N\text{-}2,6\text{-}^iPr_2\text{-}C_6H_3)(OPh)$ (**15**) required elevated temperatures (75 °C) to occur in a commensurate timeframe. Both **14** and **15** were obtained in good isolated yield.

Scheme 1. Salt metathesis route to substituted U^V-imido organometallics.

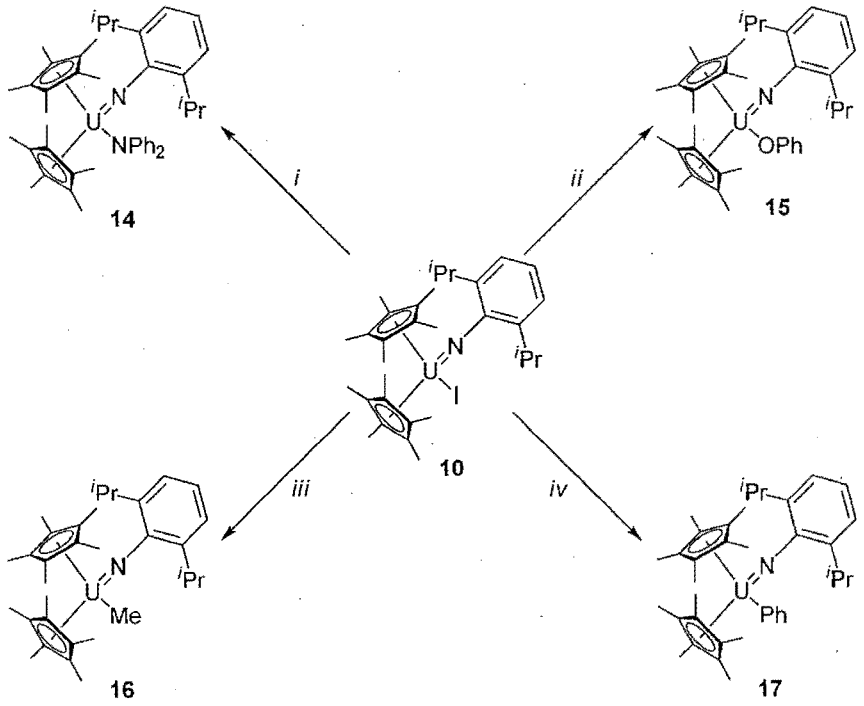

i: 1.2 equiv $KNPh_2$, 25 °C, 12 h, 80%; *ii*: 1.2 equiv KOPh, 75 °C, 12 h, 75%; *iii*: 1.5 equiv Me_2Mg(1,4-dioxane), 1,4-dioxane, 25 °C, 12 h, 70%; *iv*: 2.0 equiv $Ph_2Mg(THF)_2$, 1,4-dioxane, toluene, 25 °C, 12 h, 80%.

The molecular structure of **14** was confirmed by single-crystal X-ray diffraction (Figure 1);[40] the metrical parameters of which agree well with those observed for complexes **11** and **12**. Further, the U-N_{imido} distance and U=N-C_{Ar} angle of 1.984(4) Å and 174.0(3)° for **14** are in good agreement with those

found for the other U^V-imido complexes.[32] At 2.322(4) Å, the U(1)-N(1) bond in **14** compares well with the geometric parameters obtained for other neutral ($(Me_3Si\text{-}N=)U[N(SiMe_3)_2]_3$, $U\text{-}N_{amide}$ = 2.295(10) Å),[19a] anionic ($[U(dbabh)_6]^-$, $U\text{-}N_{amide}$ = 2.23-2.27 Å) [12] and cationic ($[(C_5Me_5)U(NMe_2)_3(THF)]^+$, $U\text{-}N_{amide}$ = 2.25-2.35 Å; $[(C_5Me_5)_2U(NEt_2)_2]^+$, $U\text{-}N_{amide}$ = 2.16-2.17 Å)[20a] uranium(V) complexes containing an $U\text{-}N_{amide}$ linkage.[41]

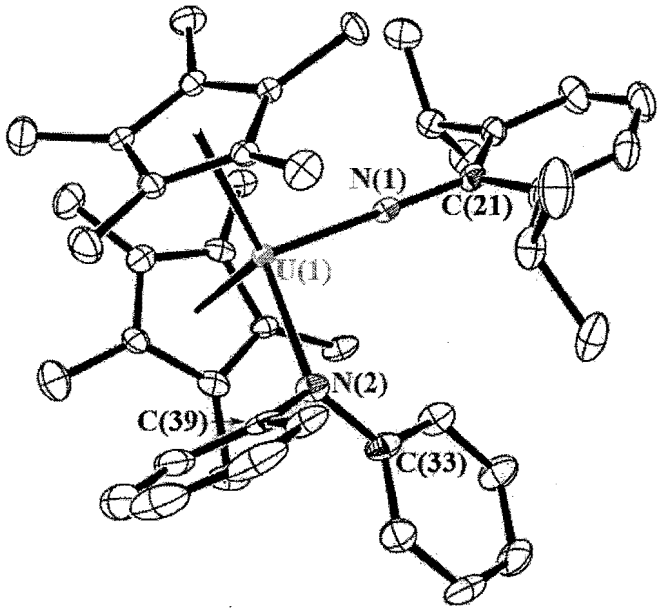

Figure 1. Molecular structure of complex **14** with thermal ellipsoids projected at the 50% probability level.

Complex **10** also served as a useful platform for the synthesis of both U^V-imido alkyl and aryl compounds — reaction between **10** and either $Me_2Mg(1,4\text{-dioxane})$ or $Ph_2Mg(THF)_2$ afforded the alkyl ($(C_5Me_5)_2U(=N\text{-}2,6\text{-}^iPr_2\text{-}C_6H_3)(Me)$ (**16**)) and aryl ($(C_5Me_5)_2U(=N\text{-}2,6\text{-}^iPr_2\text{-}C_6H_3)(Ph)$ (**17**)) complexes, respectively, in good isolated yield (Scheme 1). Paired with **13**, the isolation of **16** and **17** show that the uranium complex can host the full range of carbon anions (sp, sp^2 and sp^3), and are, to the best of our knowledge, the first examples of pentavalent uranium complexes with anionic carbon ligands other than a carbocyclic (C_5R_5, C_7H_7, C_8H_8) ligand.

C – Protonolysis and Insertion

$(C_5Me_5)_2U(=N\text{-}2,6\text{-}^iPr_2\text{-}C_6H_3)(Me)$ (**16**) and $(C_5Me_5)_2U(=N\text{-}2,6\text{-}^iPr_2\text{-}C_6H_3)(Ph)$ (**17**) served as useful starting materials for the synthesis of the U^V-imido ketimide complex $(C_5Me_5)_2U(=N\text{-}2,6\text{-}^iPr_2\text{-}$

C_6H_3)(N=CPh_2) (**18**) (Scheme 2). *In situ*-formed **16** was heated at 75 °C in the presence of excess benzophenone imine to afford **18** in good isolated yield (86%) by protonolysis and concomitant loss of methane. Alternatively, insertion of benzonitrile into the U-C_{aryl} bond in *in situ*-formed **17** gave the identical product **18** in 91% yield. These pathways not only extend the scope of this U^V-imido chemistry, but they also help confirm the existence of both **16** and **17**, which were not structurally characterized.

Scheme 2. Protonolysis routes from U^V-imido alkyl/aryl complexes toward $(C_5Me_5)_2U$(=N-2,6-^{i}Pr$_2$-C_6H_3)(N=CPh_2) (**18**).

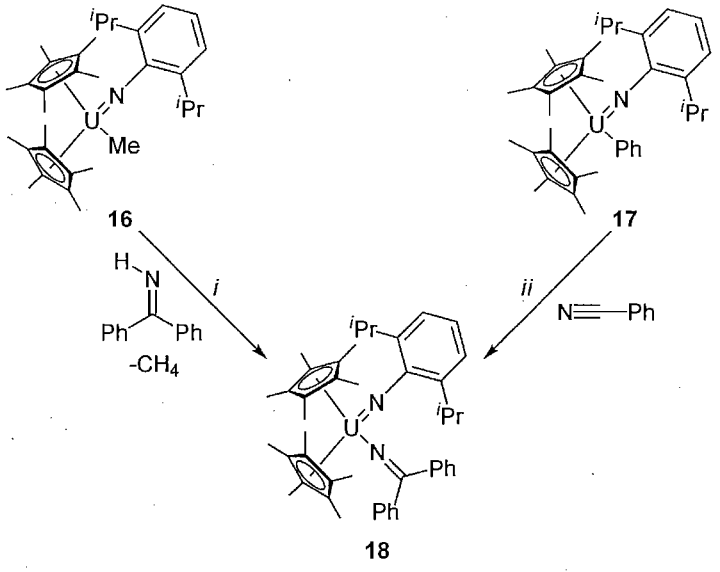

i: 1.2 equiv benzopehone imine, 75 °C, 12 h, 86%; *ii*: 1.2 equiv benzonitrile, 12 h, 91%.

Single crystals of **18** suitable for X-ray diffraction studies were obtained by slow evaporation of a concentrated solution of hexamethyldisiloxane at room temperature. Complex **18** (Figure 2) represents the first uranium-ketimide complex with the metal in a formal oxidation state other than U^{IV}. As with complexes **11-15**, **18** has a nearly linear U=N-C_{Ar} angle (C(21)-N(1)-U(1) = 174.6(4)°) and a short U=N_{imido} bond distance (U(1)-N(1) = 2.012(4) Å). The U-$N_{ketimide}$ bond length (U(1)-N(2) = 2.199(4) Å) and nearly linear U-N=C bond angle (U(1)-N(2)-C(33) = 178.2(5)°) found in **18** are comparable to those found for the structurally characterized uranium(IV) ketimide complexes (U-$N_{ketimide}$ = 2.179(6)–2.220(3) Å.[9,42-47]

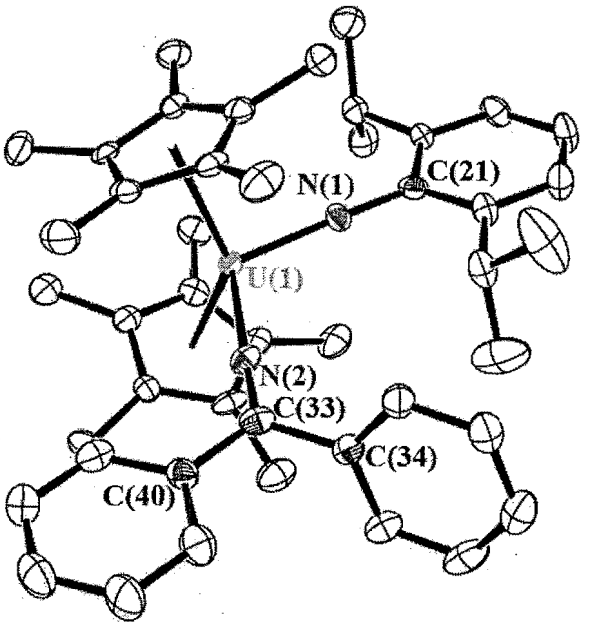

Figure 2. Molecular structure of complex **18** with thermal ellipsoids projected at the 50% probability level.

Magnetic Susceptibility.

The magnetic response of the $(C_5Me_5)_2U(=N\text{-}2,6\text{-}^iPr_2\text{-}C_6H_3)(Y)$ complexes **11-15** and **18** was measured between 2 and 350 K to evaluate changes in the electronic structure based on substitution of the auxiliary ligand. With μ_{eff} (μ_B/U) values of 2.65 (**11**), 2.48 (**12**), 2.22 (**13**), 2.27 (**14**), 2.38 (**15**) and 2.03 (**18**) the U^V-imido complexes exhibit magnetic susceptibilities similar to those observed for their U^V–imido halide counterparts[29] and other reported pentavalent uranium complexes.[19b,15,48-52] No significant differences between μ_{eff} values or temperature dependencies were observed for these complexes regardless of the identity of Y. Plots of both the χT product versus T and constant temperature magnetization (M versus H) at 2 K are provided as Supporting Information.

^{1}H NMR Spectroscopy.

The ^{1}H NMR of the uranium(V) complexes **11-13** and **15-18**[53] are similar to those found for the U^V-imido halides — they exhibit a signal corresponding to the C_5Me_5 ligand protons and an inequivalency of the *ortho* ^{i}Pr groups not seen for the U^{IV} imido starting material.[23] As has been observed for other paramagnetic uranium systems,[54] there is a dependence on the chemical shift for like protons (i.e. the C_5Me_5 resonances) and the identity of the donating ligand (X or Y) in the paramagnetic $(C_5Me_5)_2U(=N\text{-}$

2,6-$^{i}Pr_2$-C_6H_3)(X/Y) structure (Table 2). While the exact reasons for this phenomena have been debated,[55-57] it has been proposed for the uranium systems that the trend tracks with the amount of π-donation from the X/Y ligand to the metal center.[54a,c] In effect, the better the π-donor, the more electron-rich the uranium center, manifesting in a larger shielding and an upfield shift of the auxiliary protons. In this regard, the position of a set of like-protons for structurally related uranium complexes (in this present case $(C_5Me_5)_2U$(=N-2,6-$^{i}Pr_2$-C_6H_3)(X/L)) tracks with the electron density at the metal center as a result of the change in coordination environment in the complex. Therefore, **11** (L = OTf), which has the most downfield shifted $C_5\mathit{Me}_5$ resonance at δ 5.98 ppm, has the most electron deficient uranium center, presumably arising from poor donation from the OTf ligand. The $C_5\mathit{Me}_5$ shifts for the halide series vary systematically with the identity and π-donating ability of the halide ligand: **10** (X = I, δ 5.78 ppm) → **9** (X = Br, δ 5.31 ppm) → **8** (X = Cl, δ 4.92 ppm) → **7** (X = F, δ 3.94 ppm), confirming that while fluorine is the most electron negative substituent, it is the strongest π-donor compared to the other halogens. The chemical shift for the $C_5\mathit{Me}_5$ protons in **12** (δ 4.57 ppm) intersects the halide series, indicating that while the SPh group is a better donor than the larger halides, fluorine is still a better π-donor. The $C_5\mathit{Me}_5$ resonance for $(C_5Me_5)_2U$(=N-2,6-$^{i}Pr_2$-C_6H_3)(C≡C-Ph) (δ 4.11 ppm) is slightly less that of **7**, which is not surprising given that while the C≡C-Ph fragment is a strong σ–donor, its ability to π–donate should be minimal. The $C_5\mathit{Me}_5$ resonance for $(C_5Me_5)_2U$(=N-2,6-$^{i}Pr_2$-C_6H_3)(OPh) (δ 3.33 ppm) is further upfield, and the U^{V}-imido ketimide complex **18** is shifted to the largest upfield position: δ 1.41 ppm. Paired with the geometric parameters, this peak position implies that the ketimide ligand is strongly donating to the uranium center, consistent with previous studies that suggest that a bond order greater than one exists between the uranium and $N_{ketimide}$.[9,44] Interestingly, both the Me (δ 3.30 ppm) and Ph (δ 3.00 ppm) ligands are also strongly donating to the uranium center in this system, to an extent approximately equal to or slightly better than the alkoxide derivative. Overall, given the relative positions of the $C_5\mathit{Me}_5$ resonances for the U^{V}-imido complexes, the trend in increasing π-donating ability for the X/L ligand is OTf < I < Br < Cl < SPh < C≡C-Ph < F < OPh ~ Me < Ph << N=CPh_2. This

is in accord with electrochemistry data which suggest a similar trend in ease of oxidation across the series (*vide infra*).

Table 2. ^{1}H NMR Chemical Shift of the C_5Me_5 Protons in the $(C_5Me_5)_2U(=N\text{-}2,6\text{-}^iPr_2\text{-}C_6H_3)(X/Y)$ Complexes at 25 °C in C_6D_6.

Compound	δ (ppm)	Compound	δ (ppm)
7 (X = F)	3.94	**12** (Y = SPh)	4.57
8 (X = Cl)	4.92	**13** (Y = C≡CPh)	4.11
9 (X = Br)	5.31	**15** (Y = OPh)	3.33
10 (X = I)	5.78	**16** (Y = Me)	3.30
11 (Y = OTf)	5.98	**17** (Y = Ph)	3.00
		18 (Y = N=CPh$_2$)	1.41

Electrochemistry.

Cyclic and square-wave voltammetric data have been collected for $(C_5Me_5)_2U(=N\text{-}2,6\text{-}^iPr_2\text{-}C_6H_3)(X/L)$ complexes **7-16** and **18** in ~ 0.1 M [Bu_4N][fluoroarylborate]/tetrahydrofuran solution ([fluoroarylborate]$^-$ = $[B(C_6F_5)_4]^-$ or $[B(3,5\text{-}(CF_3)_2\text{-}C_6H_3)_4]^-$). The potential data are summarized in Table 3, and typical cyclic voltammograms are illustrated in Figure 3. Data for **7-10**[29] and **13**[31] have been previously reported, but are included here for completeness. We were unable to obtain voltammetric data for **17** because of very rapid decomposition of this complex in the supporting electrolyte solution. Similar problems were encountered previously for the fluoride complex (**7**),[29] and low-temperature voltammetry was found sufficient to stabilize that complex for data collection. Similar efforts were not made for **17**.

The voltammetric data for the new U^V-imido complexes (**11**, **12**, **14-16**, **18**) are completely consistent with that reported previously for the halides (**7-10**) and the acetylide complex (**13**). In particular, all these systems exhibit two chemically reversible one-electron redox transformations; an oxidation wave attributable to the U^{VI}/U^V process and a reduction wave attributable to the U^V/U^{IV} process. As illustrated in Figure 3, the separations between the anodic and cathodic peaks for these waves deviate, in some cases substantially, from the nominal electrochemically reversible value of 60 mV indicating that the heterogeneous electron-transfer rates vary significantly across this series.[58] This behavior was

reported previously for the halide complexes.[29] Of greater interest is the variability in the half-wave potentials for these metal-based redox transformations across this series reflecting the role of the ancillary ligand in perturbing the redox energetics in these systems (Table 3). This perturbation appears to derive from an interplay between purely electrostatic effects (e.g., for the triflate complex **11**) and more intrinsic σ- and π-bonding interactions that shift electron density at the metal center thereby impacting the redox energetics. The overall effect across the series is quite dramatic for a seemingly small structural perturbation to the otherwise constant U^{V}-imido core (Table 1). If one considers the potential of the U^{VI}/U^{V} oxidation wave, the process shifts by ~ 0.7 V on going from the triflate complex (**11**) to the ketimide complex (**18**). As noted above, the chemical shift of C_5Me_5 ligand protons in the ^{1}H NMR spectra (Table 2) reflects the extent of π-donation from the ancillary ligand to the metal center. Interestingly, there is an excellent linear correlation between these chemical shift values and the oxidation potentials (Figure 4), suggesting that there is a common origin, π-donation from the ligand to the metal, contributing to both observables.

Finally, we note that the nearly constant potential separation between the U^{VI}/U^{V} and U^{V}/U^{IV} couples described previously[29] is retained across this entire series of eleven complexes, with an average $|\Delta E_{1/2}|$ value of 1.52 ± 0.03 V. This implies that the factors responsible for (de)stabilizing the oxidation process are equally at play in shifting the reduction wave in the same direction. Thus, for example, the π-donor ligands stabilize the U^{VI} oxidation state while concomitantly destabilizing the more electron-rich U^{IV} oxidation state by an approximately equal amount.

Table 3. Summary of Redox Potential Data[a] for the $(C_5Me_5)_2U((=N\text{-}2,6\text{-}^iPr_2\text{-}C_6H_3)(X/Y)$ Complexes **7-16** and **18** in ~0.1 M $[Bu_4N][fluoroarylborate]^-$[b]/THF Solution at Room Temperature.

U^V Complexes	X	Electrolyte Anion[b]	$E_{1/2}$ (U^{VI}/U^V) (V)	$E_{1/2}$ (U^V/U^{IV}) (V)	$\|\Delta E_{1/2}\|$ (V)	Ref.
7[c]	F	BAr_F	-0.14	-1.81	1.67	29
8	Cl	BAr_F	0.03	-1.52	1.55	29
9	Br	BAr_F	0.07	-1.44	1.51	29
10	I	$B(C_6F_5)_4$	0.11	-1.37	1.48	28,29
11	OTf	BAr_F	0.36	-1.21	1.57	28, this work
12	SPh	BAr_F	0.00	-1.43	1.43	28, this work
13	C≡CPh	BAr_F	-0.10	-1.64	1.54	31
14	NPh_2	BAr_F	-0.30	-1.65	1.35	this work
15	OPh	BAr_F	-0.22	-1.75	1.53	this work
16	Me	BAr_F	-0.13	-1.71	1.58	this work
18	$N{=}CPh_2$	BAr_F	-0.34	-1.84	1.50	this work
				$\|\Delta E_{1/2}\|_{(ave)}$	1.52 ± 0.03	
U^{IV} Precursor	L	Electrolyte Anion[b]	$E_{1/2}$ (U^V/U^{IV}) (V)	$E_{1/2}$ (U^{IV}/U^{III}) (V)	$\|\Delta E_{1/2}\|$ (V)	
2[d]	THF	BAr_F	-0.86	-2.40	1.54	28

[a]All $E_{1/2}$ values are versus $[(C_5H_5)_2Fe]^{+/0}$ and were determined from the peak position in a square-wave voltammogram or from the average of the cathodic and anodic peaks in a cyclic voltammogram. [b]Electrolyte anion was either $[B(3,5\text{-}(CF_3)_2\text{-}C_6H_3)_4]^-$ (BAr_F), or $[B(C_6F_5)_4]^-$. [c]Although scan-rate dependent behavior was explored at ~-50 °C, potential calibration data were collected for this complex at room temperature using a freshly prepared solution.

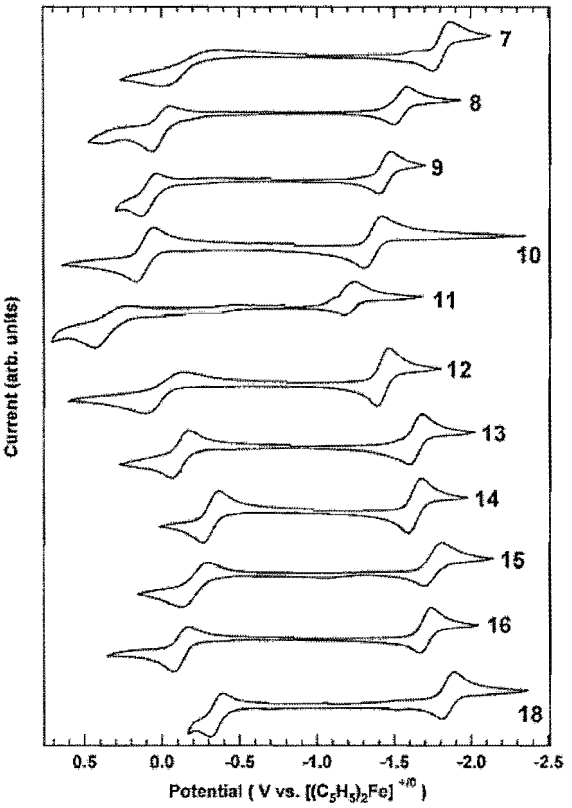

Figure 3. Cyclic voltammograms for the $(C_5Me_5)_2U(=N\text{-}2,6\text{-}^iPr_2\text{-}C_6H_3)(X/Y)$ complexes **7**-**16** and **18** in ~ 0.1M $[Bu_4N]$[fluoroarylborate]/THF solution at 200 mV/s scan rate at a Pt electrode.

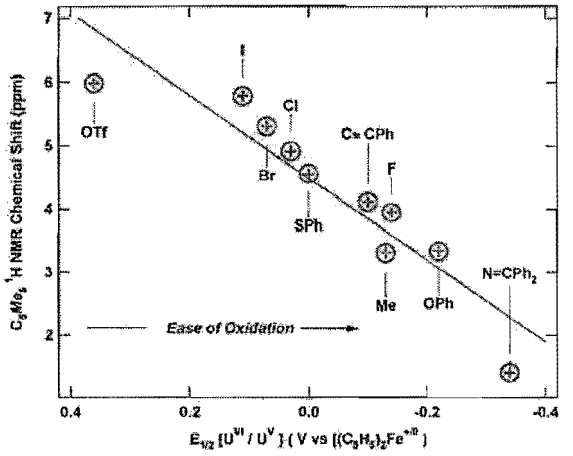

Figure 4. Linear correlation between ^1H NMR chemical shift of the C_5Me_5 protons and oxidation potential for $(C_5Me_5)_2U(=N\text{-}2,6\text{-}^iPr_2\text{-}C_6H_3)(X/Y)$. The correlation includes all ten available data points ($R^2 = 0.93$).

Electronic Spectroscopy.

As noted previously,[29,31] the organometallic U^V-imido complexes provide an excellent opportunity to explore in detail the electronic/molecular structure relationship. Their simple $5f^1$ valence electronic configuration gives rise to relatively straightforward electronic spectra, and the essentially constant molecular structural framework provided by the $(C_5Me_5)_2U(=N\text{-}2,6\text{-}^iPr_2\text{-}C_6H_3)$ core enables a focus on perturbations introduced by the ancillary ligand (X/Y) in the metallocene wedge. Additionally, the imido ligand with its covalent multiple bonding to the metal center introduces additional molecular electronic states of both ligand-localized and charge-transfer character that have the potential to interact with the ligand-field (f-f) states in ways that provide additional diagnostics for the electronic structure and electronic interactions in these systems.

Consideration of the electronic spectra begins by examining the entire UV-visible-near IR region illustrated in Figure 5. For comparison purposes we have also included previously published spectra for complexes **7**-**10**[29] and **13**.[31] There is remarkable consistency in the spectral band shapes and intensities, particularly for the spectra in the upper panel of Figure 2. The variability is somewhat greater in the spectra in the lower panel, although it should be noted that the intensity data for the methyl (**16**) and phenyl (**17**) complexes are less certain because these samples were prepared from material that was of an oily consistency that made accurate weighing problematic. The spectral assignments for the bands in the region from 10 000 – 33 000 cm^{-1} have been described in detail previously and derive principally from transitions localized on the $(C_5Me_5)_2U(=N\text{-}2,6\text{-}^iPr_2\text{-}C_6H_3)$ core.[29] Given the correlations among these spectra, it is likely that these assignments remain valid for all these complexes. Specifically, the lowest energy broad bands at ~ 10000 and 14000 cm^{-1} are assigned to the two different spin components of the imido-to-metal charge-transfer transition; $^4(\pi_{M=N}\rightarrow nb_{5f})$ and $^2(\pi_{M=N}\rightarrow nb_{5f})$, respectively (nb = non-bonding). The higher energy bands in the UV-visible region are comprised at least in part of $\pi_{M=N}\rightarrow\pi^*_{Ph}$ transitions. These assignments are all supported by density functional theory calculations.[29] The strong spectral correlation across most of this series suggests that the ancillary (X/Y) ligand does not contribute significantly to electronic excited states within the region probed in our studies. The

exceptions to this observation appear to be in the spectra for the acetylide (**13**) and ketimide (**18**) as evidenced by the substantially larger transition intensity in the higher energy region. Both of these ligands possess low-energy non-bonding, π and/or π* orbitals that should contribute to the spectral density of states in this region.[4,5,59,60] This becomes significant in the context of the f-f transition intensities discussed below.

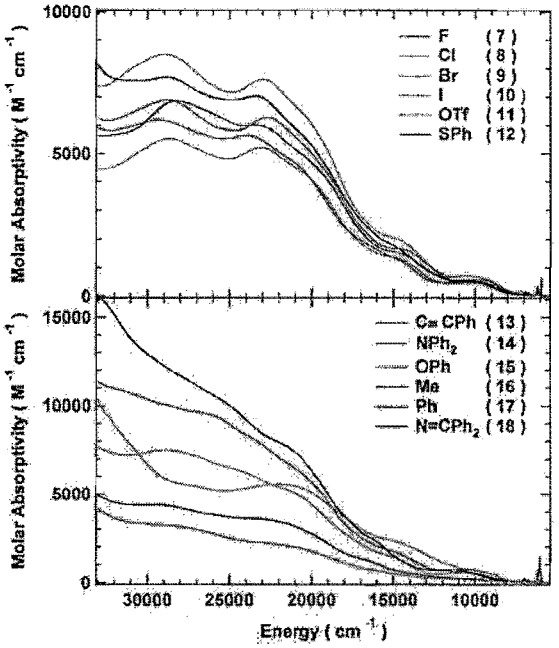

Figure 5. UV-visible-NIR electronic absorption spectra of the $(C_5Me_5)_2U(=N\text{-}2,6\text{-}^iPr_2\text{-}C_6H_3)(X/Y)$ complexes **7**-**18** in toluene solution at room temperature.

The $5f^1$ valence electronic configuration in all these complexes gives rise to a fairly simple f-orbital density of states. Spin-orbit coupling leads to only two manifolds of states; a $^2F_{5/2}$ ground-state manifold and a $^2F_{7/2}$ excited-state manifold. These manifolds will be further split according to the symmetry and strength of the crystal field imposed by the ligand environment. In the low symmetry of these U^V-imido complexes (nominally C_s symmetry), all orbital degeneracies should be removed leading to a total of seven states and six possible transitions. (Note that each state will still be a Kramer doublet as a consequence of the odd electron count.) Preliminary ligand-field calculations incorporating spin-orbit coupling reported by us previously[29] for structurally simplified surrogates of the fluoride (**7**) and iodide (**10**) complexes are in general good agreement with published data and interpretations for $5f^1$ systems in higher symmetry (e.g., *pseudo*-octahedral) environments such as the U^V hexahalides.[18]

Specifically, our calculations predict that two transitions lie within ~2800 cm^{-1} of the ground-state and would not be observable in our experiments. The four remaining transitions are predicted to lie 6000 – 10 000 cm^{-1} above the ground state, with the two lowest levels occurring at 6200 and 7100 cm^{-1}.

A set of narrow, lower intensity bands in this low energy spectral region is readily discernible in the data shown in Figure 5. These bands were isolated for better interpretation and comparison by fitting a Gaussian profile to the broad band at 10 000 cm^{-1} and subtracting this broad band from the lower energy region. In addition, for several of the complexes, data were collected at 77 K in a toluene-d_8 glass to enhance the spectral resolution. Typical data for these f-f bands after this higher-energy background subtraction routine are illustrated in Figures 6 and 7. The spectra clearly are comprised of many bands resulting from both pure electronic transitions and vibronic transitions built on the electronic transitions. At a qualitative level, the spectral data for all twelve complexes appear to be comprised of two sets of bands. The first set occurs in the same energy range (with the most prominent band at ~6000–6200 cm^{-1}) for all complexes. The second set establishes some distinction among the complexes. For the fluoride (**7**), amide (**14**), and phenoxide (**15**) the second set begins with the most prominent band at ~7300 cm^{-1}, whereas for all other complexes, this second set begins with the most prominent band occurring at lower energy (~6800–7000 cm^{-1}). Note, however, that these ranges are in good agreement for all complexes with prediction from the ligand field/spin orbit calculations performed previously for the fluoride and iodide model systems $(C_5Me_5)_2U(=N\text{-}C_6H_5)(X)$ (X = F, I).[29]

Examination of the 77 K data (Figure 6) in this f-f spectral region for the four halide complexes provides some quantitative support for the interpretation that this region is comprised of *two* different sets of electronic transitions each of which has vibronic structure (instead of a single electronic transition with vibronic structure). First, as previously noted,[29] there is a very weak feature in the room temperature data for each of the halide complexes at ~5900 cm^{-1} that disappears in the 77 K spectra. This indicates that this feature is a vibronic hot-band, and therefore the most intense band in the 6100–6200 cm^{-1} region is an electronic origin. (Note that there is no inversion symmetry in these complexes, so dipole-selection rules associated with orbital parity are relaxed.) Next, the series of weak bands in

the region just above this very intense feature (~6360, 6520, and 6590 cm^{-1}) is nearly identical for the chloride, bromide, and iodide complexes (with very minor shifts of all bands to slightly higher energy along the series Cl < Br < I) consistent with vibronic structure derived from vibrational modes of nearly identical energy for all three complexes. Since these features occur at nearly the same energy in all three spectra, they likely derive from modes localized on the $(C_5Me_5)_2U(=N\text{-}2,6\text{-}^iPr_2\text{-}C_6H_3)$ core, and do not involve the M-X bond to an appreciable extent. The spectrum of the fluoride complex also has several weak vibronic features in this same region, as expected since it, too, has this same metallocene imido framework. To higher energy, however, there is a significant difference in the spectral data for the fluoride complex versus those of the other halides, with the next distinctive feature in the fluoride spectrum lying some ~500 cm^{-1} to higher energy than those in the spectra of the other halides (~7250 cm^{-1} vs. ~6700 cm^{-1}). This strongly suggests that this next series of bands derives from a new electronic transition (and related vibronic sidebands to higher energy) that lies to higher energy in the fluoride complex than in the other halides because of the greater perturbative influence of the fluoride ion compared to that of the other halides on the metal-based energy levels.

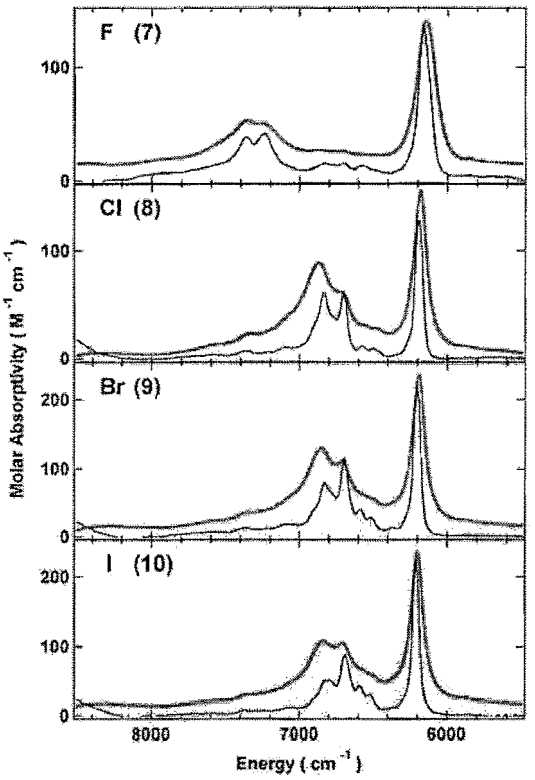

Figure 6. NIR electronic absorption spectra of the $(C_5Me_5)_2U(=N\text{-}2,6\text{-}^iPr_2\text{-}C_6H_3)(X)$ complexes **7-10** in toluene-d_8 solution at room temperature (red, offset for clarity) and 77 K (blue). Higher-energy tails from the visible spectra have been subtracted (see text).

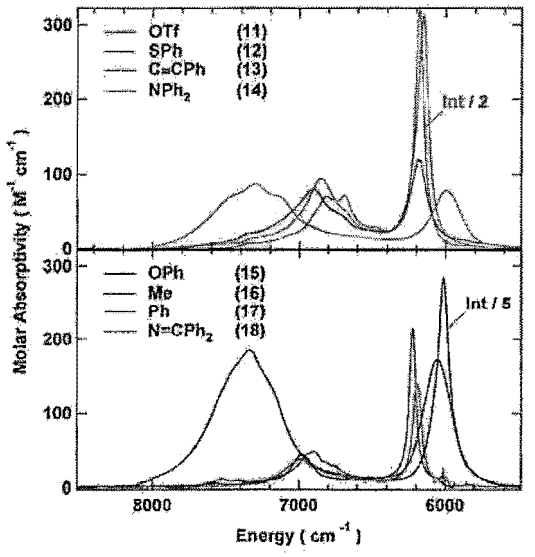

Figure 7. NIR electronic absorption spectra of the $(C_5Me_5)_2U(=N\text{-}2,6\text{-}^iPr_2\text{-}C_6H_3)(Y)$ complexes **11-18** in toluene-d_8 solution at room temperature. Higher-energy tails from the visible spectra have been subtracted (see text).

The rich vibronic structure seen at 77 K for the halide complexes is less readily discernible in the RT data for the other non-halide systems (Figure 7), but the gross spectral features clearly fall into one of two categories; those with the higher energy set of f-f bands in the same higher-energy range as those of the fluoride complex (i.e., the amide (**14**) and the phenoxide (**15**)) and those whose spectra are more like those of the heavier halides. The crystal structure data (Table 1) that span most of the twelve complexes under consideration demonstrate that all complexes have very similar structural parameters, with the only significant difference being the identity of the ancillary ligand (X/Y) in the metallocene wedge, and the metal-ligand bond distance for this ligand. It is also expected that the spin-orbit coupling constant for U^V should remain essentially constant across the entire series of complexes. Thus, the spectral data provide an important opportunity to focus specifically on the contribution of the ancillary ligand to the splitting of the f-f states in these systems. In principal, these data can be used to arrange the ancillary ligands according to a spectrochemical or nephelauxetic series.[61] However, the low symmetry of these complexes necessitates more parameters to describe the energy level splitting than can be deduced from the energies of just the two states identified in our data. We are currently pursuing additional density functional theory based calculations to enable a more quantitative assessment. It is clear that the complexes can be divided into two distinct classes based on these spectral data, and the grouping of the fluoride, amide, and phenoxide systems into the same class as suggested above is most consistent with the propensity of these ligands to interact strongly with the metal center by both σ- and π-donation that would be expected to lead to greater splitting of the $5f^1$ levels.

The final consideration regarding these f-f spectral data concerns the intensities in the absorption bands. In classical coordination compounds of pentavalent uranium in *pseudo*-octahedral symmetry, such as the hexahalides, typical molar absorptivities are in the range ~5–20 $M^{-1}cm^{-1}$.[18] In contrast, for the U^V-imido complexes herein, the molar absorptivities in the principal bands are in the range from ~100 to ~1500 $M^{-1}cm^{-1}$. Clearly some of this discrepancy can be attributed to the fact that there is a relaxation in the electric dipole selection rules for these f-f transitions as the symmetry is reduced from

pseudo-octahedral in the hexahalides to ~C_s symmetry in the imido complexes. This alone cannot account for the observed more than 20-fold difference in intensities. It is more likely that the f-f transitions in the imido complexes gain intensity by coupling to the higher lying charge-transfer states that give rise to the spectral band shown in Figure 5. Such coupling should scale according to the transition intensity in these higher lying states and their energetic proximity to the f-f transitions.[61] In support of this proposed enhancement mechanism, we note in particular that the two complexes possessing the most intense f-f bands, the acetylide (**13**) and the ketimide (**18**), are also the complexes exhibiting the greatest intensities in the UV-visible transitions (Figure 5).

Conclusions

The chemistry reported here is a valuable entry into the synthesis and characterization of pentavalent uranium organometallic complexes. The synthetic protocols developed enable for the generation of a variety of $(C_5Me_5)_2U(=N\text{-}2,6\text{-}^iPr_2\text{-}C_6H_3)(L)$ (where L = OTf, SPh, NPh_2, OPh, Me, Ph, $N{=}CPh_2$) complexes. This is a strong complement to other reported routes to U^V organometallic species, and we have demonstrated that a multitude of substitution patterns can be achieved utilizing an array of reaction pathways — direct oxidation of the U^{IV}-imido precursor, salt metathesis, protonolysis or insertion. That a wide range of substituents can be supported within the wedge of these U^V-imido complexes refutes prior assertions that pentavalent organouranium complexes are inherently unstable.

Structural analyses, electrochemical and spectroscopic studies provide a coherent description of the electronic structure of these pentavalent systems and indicate that both the U-X/Y and U=N bonds exhibit covalency. The qualitative picture of the energy levels that emerges from the absorption spectra and shows the f-f excitations occur at low energies and both charge-transfer and ligand-based excitations arise at higher energies, where the latter transitions involve excitations from M=N bonding orbitals to either 5f orbitals or ligand-based π^* orbitals. The electrochemical analysis shows that the ligand framework can stabilize both the U^{IV} and U^{VI} oxidation states.

Experimental

General Considerations

Reactions and manipulations were performed in either a recirculating Vacuum Atmospheres NEXUS model inert atmosphere (N_2) drybox equipped with a 40CFM Dual Purifier NI-Train or using standard Schlenk techniques. Glassware was dried overnight at 150 °C before use. All NMR spectra were obtained in C_6D_6 using a Bruker Avance 300 MHz spectrometer. Chemical shifts for ^{1}H NMR spectra were referenced to solvent impurities. Melting points were determined with a Melt-Temp II capillary melting point apparatus equipped with a Fluke 50S K/J thermocouple using capillary tubes flame–sealed under nitrogen; values are uncorrected. Mass spectrometric (MS) analyses were obtained at the University of California, Berkeley Mass Spectrometry Facility, using a VG ProSpec (EI) mass spectrometer. Elemental analyses were performed at the University of California, Berkeley Microanalytical Facility, on a Perkin–Elmer Series II 2400 CHNS analyzer. X-ray data were collected using either a Bruker APEX2 or Bruker P4/CCD diffractometer. Structural solution and refinement was achieved using the SHELXL97 program suite.[62] Details regarding data collection are provided in the CIF files.

Benzene-d_6 (Aldrich) was purified by passage through activated alumina and storage over activated 4Å molecular sieves prior to use. Celite (Aldrich), alumina (Brockman I, Aldrich) and 4 Å molecular sieves (Aldrich) were dried under dynamic vacuum at 250 °C for 48 h prior to use. All solvents (Aldrich) were purchased anhydrous, dried over KH for 24 h, passed through a column of activated alumina and stored over activated 4 Å molecular sieves prior to use. $(C_5Me_5)_2U(=N\text{-}2,4,6\text{-}^tBu_3\text{-}C_6H_2)$ (**1**),[30] $(C_5Me_5)_2U(=N\text{-}2,6\text{-}^iPr_2\text{-}C_6H_3)(THF)$ (**2**),[23] $Me_2Mg(1,4\text{-dioxane})$ and $Ph_2Mg(THF)_2$,[63,64] $[Bu_4N][B(C_6F_5)_4]$[65] and $[Bu_4N][B(3,5\text{-}(CF_3)_2\text{-}C_6H_3)_4]$[65] were prepared according to literature methods, and **11** and **12** were prepared as previously reported.[28] KOPh and KPh_2 were both prepared by refluxing a THF solution of HOPh and $HNPh_2$, respectively, over 1 equiv of KH for 24 h.[66]

Caution: Depleted uranium (primary isotope ^{238}U) is a weak α–emitter (4.197 MeV) with a half–life of 4.47×10^9 years; manipulations and reactions should be carried out in monitored fume hoods or in an inert atmosphere drybox in a radiation laboratory equipped with α– and β–counting equipment.

Instrumentation and Sample Protocols

Electronic absorption spectral data were obtained for toluene or toluene-d_8 solutions of complexes over the wavelength range 300–2500 nm on a Perkin-Elmer Model Lambda 950 UV–visible–NIR spectrophotometer. Room temperature data were collected in 1 cm and 1 mm path length cuvettes loaded in the Vacuum Atmospheres drybox system described above run versus the appropriate toluene solvent reference. Samples were typically run at multiple dilutions to optimize absorbance in the UV-visible and near-infrared, respectively. Data collected at 77 K were obtained from samples in toluene-d_8 contained in medium-walled NMR tubes (503-PS from Wilmad/Lab Glass). The samples were immersed in an optical dewar with a quartz cold-finger (WG-850-Q-PTI) and run in a standard transmission spectrometer configuration versus air after ensuring the solutions glassed upon freezing. Pure toluene-d_8 was run under identical conditions to perform solvent corrections to the sample spectra post-data collection. No effort was made to be quantitative in determining extinction coefficients of the samples under these conditions. Spectral resolution was typically 2 nm in the visible region and 4–6 nm in the near-infrared in all cases.

Voltammetric data were obtained in the Vacuum Atmospheres drybox system described above. In addition, data for complex **7** were obtained in a Schlenk-line electrochemical cell immersed in a dry ice/2-propanol bath at ~–50 °C. All data were collected using a Perkin-Elmer Princeton Applied Research Corporation (PARC) Model 263 potentiostat under computer control with PARC Model 270 software. All sample solutions were ~1-2 mM in complex with 0.1 M $[Bu_4N][B(3,5\text{-}(CF_3)_2\text{-}C_6H_3)_4]$ or $[Bu_4N][B(C_6F_5)_4]$ supporting electrolyte in THF solvent.[65] All data were collected with the positive-feedback IR compensation feature of the software/potentiostat activated to ensure minimal contribution to the voltammetric waves from uncompensated solution resistance (typically ~1 kΩ under the conditions employed). For experiments at ambient temperature, solutions were contained in PARC

Model K0264 microcells consisting of a ~3 mm diameter Pt disk working electrode, a Pt wire counter electrode, and a Ag wire quasi-reference electrode. For the low temperature experiment, a Schlenk cell was employed consisting of Pt wire working and counter electrodes sandwiching a Ag wire quasi-reference electrode. Scan rates from 20–5000 mV/s were employed in the cyclic voltammetry scans to assess the chemical and electrochemical reversibility of the observed redox transformations. Half-wave potentials were determined from the peak values in the square-wave voltammograms or from the average of the cathodic and anodic peak potentials in the reversible cyclic voltammograms. Potential calibrations were performed at the end of each data collection cycle using the ferrocenium/ferrocene couple as an internal standard. Electronic absorption and cyclic voltammetric data were analyzed using Wavemetrics IGOR Pro (Version 4.0) software on a Macintosh platform.

Magnetic susceptibility data were collected using a Quantum Design Superconducting Quantum Interference Device (SQUID) magnetometer at 5 T from 2-350 K. The samples were sealed in a 5mm Wilmad 505-PS NMR tube along with a small amount of quartz wool, which held the sample near the tube center. Contributions to the magnetization from quartz wool and the NMR tube were measured independently and subtracted from the total measured signal. Diamagnetic corrections were made with the use of Pascal's constants.

Synthesis of $(C_5Me_5)_2U(=N\text{-}2,6\text{-}^iPr_2\text{-}C_6H_3)(NPh_2)$ ***(14)***

A 125–mL side-arm flask equipped with a stir bar was charged with $(C_5Me_5)_2U(=N\text{-}^iPr_2\text{-}C_6H_3)(I)$ (**10**) (0.25 g, 0.31 mmol) and toluene (50 mL). $KNPh_2$ (0.077 g, 0.37 mmol) was added to the stirring dark brown solution and the reaction was stirred at room temperature. After 12 h, the reaction mixture was filtered through a Celite–padded coarse frit and volatiles were removed from the filtrate. The residue was extracted into hexanes (50 mL) and filtered through a Celite–padded coarse porosity frit. The filtrate was collected and the volatiles were removed under reduced pressure to give **14** as a brown solid (0.21 g, 0.25 mmol, 80%) suitable for further reaction. X-ray quality samples of **14** were obtained by recrystallization from a toluene/hexamethyldisiloxane (1/1) mixture at -30 °C. Anal. Calcd for $C_{44}H_{57}N_2U$ (mol. wt. 851.97): C, 62.03, H, 6.74; N, 3.29. Found: C, 61.94; H, 6.37; N, 3.54. Mp =

205-207 °C. MS (EI, 70 eV): m/z 851 (M^+). $U^{VI/V}$ $E_{1/2}$ = -0.30 V, $U^{V/IV}$ $E_{1/2}$ = -1.65 V (vs. $[(C_5H_5)_2Fe]^{+/0}$ in THF/0.1 M $[Bu_4N][B(3,5\text{-}(CF_3)_2\text{-}C_6H_3)_4]$). The ^1H NMR of **14** could not be obtained over the temperature range 0-100 °C.

Synthesis of $(C_5Me_5)_2U(=N\text{-}2,6\text{-}^iPr_2\text{-}C_6H_3)(OPh)$ (15)

A 150–mL thick-walled Schlenk tube equipped with Teflon valve and a stir bar was charged with $(C_5Me_5)_2U(=N\text{-}2,6\text{-}^iPr_2\text{-}C_6H_3)(I)$ (**10**) (0.25 g, 0.31 mmol), a magnetic stir bar, and toluene (50 mL). To the dark brown solution was added KOPh (0.049 g, 0.37 mmol) as an off-white powder. The reaction vessel was sealed and removed from the drybox to a fumehood, where it was placed in a 75 °C oil bath. After 12 h, the reaction was removed from heat, cooled to room temperature, and brought back into the drybox. The reaction was filtered though a Celite–padded coarse frit and the volatiles were removed from the filtrate. The crude product was extracted into hexanes (50 mL), filtered through a Celite–padded coarse frit, and the volatiles removed under reduced pressure to give **15** as a brown solid (0.18 g, 0.23 mmol, 75%) suitable for further reaction. X-ray quality samples of **15** were obtained by recrystallization from a concentrated hexamethyldisiloxane solution at -30 °C. ^1H NMR (C_6D_6, 298 K): δ 49.91 (b, 1H, C*H*(Me)$_2$), 22.79 (1H, Ar-*H*), 16.43 (1H, Ar-*H*), 13.56 (1H, OPh), 11.43 (6H, CH(*Me*)$_2$), 10.21 (2H, OPh), 8.54 (1H, OPh), 3.33 (30H, (C_5*Me*$_5$)$_2$), -6.19 (6H, CH(*Me*)$_2$), -6.79 (1H, OPh), -11.33 (1H, Ar-*H*), -20.09 (b, 1H, C*H*(Me)$_2$). Anal. Calcd for $C_{38}H_{52}NOU$ (mol. wt. 776.85): C, 58.75; H, 6.75; N, 1.80. Found: C, 58.74; H, 6.96; N, 2.04. Mp = 197-199 °C. MS (EI, 70 eV): m/z 776 (M^+). $U^{VI/V}$ $E_{1/2}$ = -0.22 V, $U^{V/IV}$ $E_{1/2}$ = -1.75 V (vs. $[(C_5H_5)_2Fe]^{+/0}$ in THF/0.1 M $[Bu_4N][B(3,5\text{-}(CF_3)_2\text{-}C_6H_3)_4]$).

Synthesis of $(C_5Me_5)_2U(=N\text{-}2,6\text{-}^iPr_2\text{-}C_6H_3)(Me)$ (16)

A 125–mL side-arm flask equipped with a stir bar was charged with $(C_5Me_5)_2U(=N\text{-}^iPr_2\text{-}C_6H_3)(I)$ (**10**) (0.50 g, 0.62 mmol) and toluene (50 mL). Me_2Mg(1,4-dioxane) (0.12 g, 0.84 mmol) was added to the stirring dark brown solution followed by 1,4-dioxane (~0.5 mL) and the reaction was stirred at room temperature. After 12 h, the reaction mixture was filtered through a Celite–padded coarse frit and volatiles were removed from the filtrate. The residue was extracted into hexanes (50 mL) and filtered

through a Celite–padded coarse porosity frit. The filtrate was collected and the volatiles were removed under reduced pressure to give **16** as a brown solid (0.30 g, 0.43 mmol, 70%) suitable for further reaction. ^{1}H NMR (C_6D_6, 298 K): δ 68.20 (b, 1H, C*H*(Me)$_2$), 28.57 (1H, Ar-*H*), 19.67 (1H, Ar-*H*), 15.20 (6H, CH(*Me*)$_2$), 3.30 (30H, (C_5*Me*$_5$)$_2$), -2.20 (3H, U-*Me*), -7.30 (6H, CH(*Me*)$_2$), -7.84 (1H, Ar-*H*), -16.06 (b, 1H, C*H*(Me)$_2$). Anal. Calcd for $C_{33}H_{50}NU$ (mol. wt. 698.79): C, 56.72; H, 7.21; N, 2.00. Found: C, 54.64; H, 7.07; N, 1.87. $U^{VI/V}$ $E_{1/2}$ = -0.13 V, $U^{V/IV}$ $E_{1/2}$ = -1.71 V (vs. $[(C_5H_5)_2Fe]^{+/0}$ in THF/0.1 M $[Bu_4N][B(3,5\text{-}(CF_3)_2\text{-}C_6H_3)_4]$).

Synthesis of $(C_5Me_5)_2U(=N\text{-}2,6\text{-}^iPr_2\text{-}C_6H_3)(Ph)$ ***(17)***

A 125–mL side-arm flask equipped with a stir bar was charged with $(C_5Me_5)_2U(=N\text{-}^iPr_2\text{-}C_6H_3)(I)$ (**10**) (0.50 g, 0.62 mmol) and toluene (50 mL). $Ph_2Mg(THF)_2$ (0.40 g, 1.24 mmol) was added to the stirring dark brown solution followed by 1,4-dioxane (~0.5 mL) and the reaction was stirred at room temperature. After 12 h, the reaction mixture was filtered through a Celite–padded coarse frit and volatiles were removed from the filtrate. The residue was extracted into hexanes (50 mL) and filtered through a Celite–padded coarse porosity frit. The filtrate was collected and the volatiles were removed under reduced pressure to give **17** as a brown solid (0.38 g, 0.50 mmol, 80%) suitable for further reactions. ^{1}H NMR (C_6D_6, 298 K): δ ^{1}H NMR (C_6D_6, 298 K): δ 52.71 (b, 1H, C*H*(Me)$_2$), 30.79 (1H, Ar-*H*), 24.15 (1H, Ar-*H*), 14.65 (2H, Ar-*H*), 13.98 (6H, CH(*Me*)$_2$), 8.03 (3H, Ar-*H*), 3.00 (30H, (C_5*Me*$_5$)$_2$), -3.57 (6H, CH(*Me*)$_2$), -4.72 (1H, Ar-*H*), -15.47 (b, 1H, C*H*(Me)$_2$). The instability of **17** precluded elemental analysis.

Synthesis of $(C_5Me_5)_2U(=N\text{-}2,6\text{-}^iPr_2\text{-}C_6H_3)(N{=}CPh_2)$ ***(18)***

Method A – Protonolysis: A 125–mL side-arm flask equipped with a stir bar was charged with $(C_5Me_5)_2U(=N\text{-}^iPr_2\text{-}C_6H_3)(I)$ (**10**) (0.25 g, 0.31 mmol) and toluene (50 mL). Me_2Mg(1,4-dioxane) (0.060 g, 0.42 mmol) was added followed by 1,4-dioxane (~0.25 mL) and the reaction was stirred for 12 h at room temperature. The resulting dark brown solution was filtered though a Celite–padded coarse frit. The filtrate was transferred to a 150–mL thick-walled Schlenk tube equipped with Teflon valve and a stir bar followed by benzophenone imine (0.067 g, 0.37 mmol) as a solution in toluene (5 mL).

The reaction vessel was sealed and removed from the drybox to a fumehood, where it was placed in a 75 °C oil bath. After 12 h, the reaction was removed from heat, cooled to room temperature, and brought back into the drybox. The reaction was filtered though a Celite–padded coarse frit and the volatiles were removed from the filtrate. The crude product was extracted into hexanes (50 mL), filtered through a Celite–padded coarse frit, and volatiles were removed under reduced pressure to give **18** as a brown solid (0.023 g, 0.27 mmol, 86%).

Method B – Insertion: A 125–mL side-arm flask equipped with a stir bar was charged with $(C_5Me_5)_2U(=N\text{-}^iPr_2\text{-}C_6H_3)(I)$ (**10**) (0.25 g, 0.31 mmol) and toluene (50 mL). $Ph_2Mg(THF)_2$ (0.20 g, 0.62 mmol) was added followed by 1,4-dioxane (~0.25 mL) and the reaction was stirred for 12 h at room temperature. The resulting dark brown solution was filtered though a Celite–padded coarse frit. Benzonitrile (0.038 g, 0.37 mmol) was added to the dark brown filtrate as a solution in toluene (5 mL) and the resulting reaction was stirred at room temperature. After 12 h, the reaction was filtered though a Celite–padded coarse frit and the volatiles were removed from the filtrate. The crude product was extracted into hexanes (50 mL), filtered through a Celite–padded coarse frit, and volatiles were removed under reduced pressure to give **18** as a brown solid (0.025 g, 0.28 mmol, 91%).

X-ray quality samples of **18** were obtained by recrystallization from a concentrated hexane solution at -30 °C. ^{1}H NMR (C_6D_6, 298 K): δ 46.50 (b, 1H, C*H*(Me)$_2$), 28.79 (1H, Ar-*H*), 23.81 (1H, Ar-*H*), 21.69 (1H, Ar-*H*), 11.40 (6H, CH(*Me*)$_2$), 9.61 (3H, Ar-*H*), 7.92 (4H, Ar-*H*), 1.58 (30H, (C_5*Me*$_5$)$_2$), -0.58 (2H, Ar-*H*), -2.38 (6H, CH(*Me*)$_2$), -8.17 (b, 1H, C*H*(Me)$_2$), -18.30 (1H, Ar-*H*),. Anal. Calcd for $C_{45}H_{57}N_2U$ (mol. wt. 863.98): C, 62.56; H, 6.65; N, 3.24. Found: C, 63.58; H,6.39; N, 3.57. Mp = 216-218 °C. MS (EI, 70 eV): m/z 863 (M^+). $U^{VI/V}$ $E_{1/2}$ = -0.34 V, $U^{V/IV}$ $E_{1/2}$ = -1.84 V (vs. $[(C_5H_5)_2Fe]^{+/0}$ in THF/0.1 M $[Bu_4N][B(3,5\text{-}(CF_3)_2\text{-}C_6H_3)_4]$).

Acknowledgements. For financial support of this work, we acknowledge LANL (Director's PD Fellowship to C.R.G. and E.J.S. and a Frederick Reines PD Fellowship to E.J.S.), the LANL G. T. Seaborg Institute (PD Fellowships to C.R.G. and E.J.S.; summer graduate student fellowship to A.E.V.),

the Division of Chemical Sciences, Office of Basic Energy Sciences, Heavy Element Chemistry program, and the LANL Laboratory Directed Research & Development program.

Supporting Information Available: Magnetic susceptibility data for **11-15** and **18** and crystallographic data for **14** and **18** (PDF, CIF). This material is available free of charge via the Internet at http://pubs.acs.org.

References:

(1) For a recent review of the chemistry concerning U^{III} as a reducing agent see: Evans, W. J.; Kozimor, S. A. *Coord. Chem. Rev.* **2006**, *250*, 911-935.

(2) While transition metal complexes follow the 18-electron rule, no such rule exists for the actinides. For pertinent examples, see: (a) Reynolds, L. T.; Wilkinson, G. *J. Inorg. Nucl. Chem.* **1956**, *2*, 246-253. (b) Fischer, E. O.; Hristidu, Y. *Z. Naturforsch.* **1962**, *173*, 275-276. (c) Streitwieser Jr. A.; Mueller-Westerhoff, U. *J. Am. Chem. Soc.* **1968**, *90*, 7364. (d) Avdeef, A.; Raymond, K. N.; Hodgson, K. O.; Zalkin, A. *Inorg. Chem.* **1972**, *11*, 1083-1088. (e) Maier, R.; Kanellakopulos, B.; Apostolidis, C.; Meyer, D.; Rebizant, J. *J. Alloys Compd.* **1993**, *190*, 269-271.

(3) Schelter, E. J.; Morris, D. E.; Scott, B. L.; Kiplinger, J. L. *Chem. Commun.* **2007**, 1029-1031.

(4) Schelter, E. J.; Yang, P.; Scott, B. L.; Da Re, R. E.; Jantunen, K. C.; Martin, R. L.; Hay, P. J.; Morris, D. E.; Kiplinger, J. L. *J. Am. Chem. Soc.* **2007**, *129*, 5139-5152.

(5) Schelter, E. J.; Yang, P.; Scott, B. L.; Thompson, J. D.; Martin, R. L.; Hay, P. J.; Morris, D. E.; Kiplinger, J. L. *Inorg. Chem.* **2007**, *46*, 7477-7488.

(6) Kiplinger, J. L.; Pool, J. A.; Schelter, E. J.; Thompson, J. D.; Scott, B. L.; Morris, D. E. *Angew. Chem., Int. Ed.* **2006**, *45*, 2036-2041.

(7) Jantunen, K. C.; Scott, B. L.; Kiplinger, J. L. *J. Alloys Compd.* **2007**, *444-445*, 363-368.

(8) Pool, J. A.; Scott, B. L.; Kiplinger, J. L. *J. Am. Chem. Soc.* **2005**, *127*, 1338-1339.

(9) Pool, J. A.; Scott, B. L.; Kiplinger, J. L. *Chem. Commun.* **2005**, 2591-2593.

(10) Diaconescu, P. L.; Arnold, P. L.; Baker, T. A.; Mindiola, D. J.; Cummins, C. C. *J. Am. Chem. Soc.* **2000**, *122*, 6108-6109.

(11) Mazzanti, M.; Wietzke, R.; Pecaut, J.; Latour, J.-M.; Maldivi, P.; Remy, M. *Inorg. Chem.* **2002**, *41*, 2389-2399.

(12) Meyer, K.; Mindiola, D. J.; Baker, T. A.; Davis, W. M.; Cummins, C. C. *Angew. Chem., Int. Ed.* **2000**, *39*, 3063-3066.

(13) Burns, C. J.; Eisen, M. S. Organoactinide Chemistry: Synthesis and Characterization. In *The Chemistry of the Actinide and Transactinide Elements*, 3rd ed.; Morss, L. R., Edelstein, N. M., Fuger, J., Eds.; Springer: The Netherlands, 2006; Vol. 5, pp 2799-2910, and references therein.

(14) Ephritikhine, M. *Dalton Trans.* **2006**, 2501-2516.

(15) For a review on the synthesis, stability and properties pentavalent uranium, see: Selbin, J.; Ortego, J. D. *Chem. Rev.* **1969**, *69*, 657-621.

(16) Bagnall, K. W. *Comprehensive Coordination Chemistry*; Wilkinson, G., Gillard, R. D., Mc Cleverty, J. A., Eds.; Pergamon: Oxford, 1987; Vol. 3, p 1129.

(17) For a detailed list of various U^{V} halide complexes, see: Grenthe I.; Drozdzynski, J.; Fujino, T.; Buck, E. C.; Albrecht-Schmitt, T. E.; Wolf, S. F. Uranium. In *The Chemistry of the Actinide and Transactinide Elements*, 3rd ed.; Morss, L. R., Edelstein, N. M., Fuger, J., Eds.; Springer: The Netherlands, 2006; Vol. 1, pp 501-529.

(18) Ryan, J. L. *J. Inorg. Nucl. Chem.* **1971**, *33*, 153-177.

(19) For representative examples of U^{V}-amide and alkoxide/aryloxide complexes, see: (a) Zalkin, A.; Brennan, J. G.; Andersen, R. A. *Acta Cryst.* **1988**, *C44*, 1553-1554. (b) Roussel, P.; Hitchcock, P. B.; Tinker, N. D.; Scott, P. *Inorg. Chem.* **1997**, *36*, 5716-5721. (c) Castro-Rodriguez, I.; Olsen, K.; Meyer, K. *J. Am. Chem. Soc.* **2003**, *125*, 4564-4571. (d) Salmon, P.; Thuery, P.; Ephritikhine, M. *Polyhedron* **2007**, *26*, 631-636. (e) Hayton, T. W.; Wu, G. *J. Am. Chem. Soc.* **2008**, *130*, 2005-2014.

(20) For examples of pentavalent organouranium complexes, see: (a) Boisson, C.; Berthet, J. -C.; Lance, M.; Nierlich, M.; Vigner, J.; Ephritikhine, M. *J. Chem. Soc., Chem. Commun.* **1995**, 543-544. (b) Gourier, D.; Caurant, D. *Inorg. Chem.* **1997**, *36*, 5931-5936. (c) Ephritikhine, M.; Berthet, J. C.; Boisson, C.; Lance, M.; Nierlich, M. *J. Alloys Compd.* **1998**, *271-273*, 144-149. (d) Boaretto, R.; Roussel, P.; Alcock, N. W.; Kingsley, A. J.; Munslow, I. J.; Sanders, C. J.; Scott, P. *J. Organomet Chem.* **1999**, *591*, 174-184. (e) Arliguie, T.; Rourmigue, M.; Ephritikhine, M. *Organometallics* **2000**, *19*, 109-111.

(21) Boisson, C.; Berthet, J.-C.; Lance, M.; Vigner, J.; Nierlich, M.; Ephritikhine, M. *J. Chem. Soc., Dalton Trans.* **1996**, 947-953.

(22) Berthet, J. C.; Ephritikhine, M. *J. Chem. Soc., Chem. Commun.* **1993**, 1566-1567.

(23) Arney, D. S. J.; Burns, C. J. *J. Am. Chem. Soc.* **1993**, *115*, 9840-9841.

(24) Brennan, J. G.; Andersen, R. A. *J. Am. Chem. Soc.* **1985**, *107*, 514-516.

(25) Castro-Rodriguez, I.; Nakai, H.; Meyer, K. *Angew. Chem., Int. Ed.* **2006**, *45*, 2389-2392.

(26) Roussel, P.; Boaretto, R.; Kingsley, A. J.; Alcock, N. W.; Scott, P. *J. Chem. Soc., Dalton Trans.* **2002**, 1423-1428.

(27) Although silver salts are among the most widely utilized oxidants for metal complexes, their behavior can be difficult to predict and control. For an excellent review on chemical oxidants for organometallic systems, see: Connelly, N. G.; Geiger, W. E. *Chem. Rev.* **1996**, *96*, 877-910.

(28) Graves, C. R.; Scott, B. L.; Morris, D. E.; Kiplinger, J. L. *J. Am. Chem. Soc.* **2007**, *129*, 11914-11915.

(29) Graves, C. R.; Yang, P.; Kozimor, S. A.; Vaughn, A. E.; Clark, D. L.; Conradson, S. D.; Schelter, E. J.; Scott, B. L.; Thompson, J. D.; Hay, P. J.; Morris, D. E.; Kiplinger, J. L. *J. Am. Chem. Soc.* **2008**, *130*, 5272-5285.

(30) Arney, D. S. J.; Burns, C. J. *J. Am. Chem. Soc.* **1995**, *117*, 9448-9460.

(31) Graves, C. R.; Scott, B. L.; Morris, D. E.; Kiplinger, J. L. *Organometallics* **2008**, *27*, 3335-3337.

(32) For other examples of imido complexes featuring short U=N_{Ar} bond distances (Å) and nearly linear U-N-C imido angles (°), see: (a) Brennan, J. G.; Andersen, R. A. *J. Am. Chem. Soc.* **1985**, *107*, 514-516. (b) Stewart, J. L. Tris[bis(trimethylsilyl)amido]uranium: Compounds with Tri-, Tetra-, and Pentavalent Uranium. Ph. D. Dissertation, University of California, Berkeley, CA, 1988. (c) Arney, D. S. J.; Burns, C. J.; Smith, D. C. *J. Am. Chem. Soc.* **1992**, *114*, 10068-10069. (d) Hayton, T. W.; Boncella, J. M.; Scott, B. L.; Palmer, P. D.; Batista, E. R.; Hay, P. J. *Science* **2005**, *310*, 1941-1943. (e) Hayton, T. W.; Boncella, J. M.; Scott, B. L.; Batista, E. R.; Hay, P. J. *J. Am. Chem. Soc.* **2006**, *128*, 10549-10559. (f) Spencer, L. P.; Yang, P.; Scott, B. L.; Batista, E. R.; Boncella, J. M. *J. Am. Chem. Soc.* **2008**, *130*, 2930. Also see references 23 and 30.

(33) Kiplinger, J. L.; John, K. D.; Morris, D. E.; Scott, B. L.; Burns, C. J. *Organometallics* **2002**, *21*, 4306-4308.

(34) Berthet, J. C.; Lance, M.; Nierlich, M.; Ephritikhine, M. *Chem. Commun.* **1998**, 1373-1374.

(35) Berthet, J. C.; Nierlich, M.; Ephritikhine, M. *Eur. J. Inorg. Chem.* **2002**, 850-858.

(36) Arliguie, T.; Fourmigue, M.; Ephritikhine, M. *Organometallics* **2000**, *19*, 109-111.

(37) Belkhiri, L.; Arliguie, T.; Thuery, P.; Fourmigue, M.; Boucekkine, A.; Ephritikhine, M. *Organometallics* **2006**, *25*, 2782-2795.

(38) U-S distances in the range of ~2.6-2.8 Å have been reported for tetravalent uranium complexes. For examples see: (a) Clark, D. L.; Miller, M. M.; Watkin, J. G. *Inorg. Chem.* **1993**, *32*, 772-774. (b) Leverd, P. C.; Ephritikhine, M.; Lance, M.; Vigner, J.; Nierlich, M. *J. Organomet. Chem.* **1996**, *507*, 229-237. (c) Lescop, C.; Arliguie, T.; Lance, M.; Nierlich, M.; Ephritikhine, M. *J. Organomet. Chem.* **1999**, *580*, 137-144. (d) Diaconescu, P. L.; Arnold, P. L.; Baker, T. A.; Mindiola, D. J.; Cummins, C. C. *J. Am. Chem. Soc.* **2000**, *122*, 6108-6109. (e) Arliguie, T.; Lescop, C.; Ventelon, L.; Leverd, P. C.; Thuery, P.; Nierlich, M.; Ephritikhine, M. *Organometallics* **2001**, *20*, 3698-3703.

(39) Experiments done on an NMR scale indicated that the corresponding Cl (**8**), Br (**9**) and OTf (**11**) complexes can also serve as starting materials for this salts metathesis route.

(40) While publication quality data for the structure of **15** was not obtained, collected data showing connectivity consistent with the molecular framework of $(C_5Me_5)_2U(=N\text{-}2,6\text{-}^iPr_2\text{-}C_6H_3)(OPh)$ was obtained. See the Supporting Information for a thermal ellipsoid plot.

(41) The $U\text{-}N_{amide}$ bond length for **14** also compares well to $U\text{-}N_{amide}$ bond lengths for tri-, tetra- and hexavalent uranium complexes containing a uranium amide linkage. (a) $U[N(SiMe_3)_2]_3$, $U\text{-}N_{amide}$ = 2.320(4) Å: Stewart, J. L.; Andersen, R. A. *Polyhedron* **1998**, *17*, 953-958. (b) $(C_5Me_5)_2U[N(SiMe_3)_2]_2$, $U\text{-}N_{amide}$ = 2.352(2) Å: Evans, W. J.; Nyce, G. W.; Forrestal, K. J.; Ziller, J. W. *Organometallics* **2002**, *21*, 1050-1055. (c) $(C_5Me_5)_2U[NH(2,6\text{-}Me_2\text{-}C_6H_3)]_2$, $U\text{-}N_{amide}$ = 2.276(6) Å: Straub, T.; Frank, W.; Reis, G. J.; Eisen, M. S. *J. Chem. Soc., Dalton Trans.* **1996**, 2541-2546. (d) $[N(SiMe_3)_2]_3U(=N\text{-}SiMe_3)(F)$, $U\text{-}N_{amide}$ = 2.217(17)-2.252(17) Å; $[N(SiMe_3)_2]_3U(=N\text{-}C_6H_5)(F)$: $U\text{-}N_{amide}$ = 2.206(7)-2.226(6) Å: Burns, C. J.; Smith, W. H.; Huffman, J. C.; Sattelberger, A. P. *J. Am. Chem. Soc.* **1990**, *112*, 3237-3238.

(42) Diaconescu, P. L.; Cummins, C. C. *J. Am. Chem. Soc.* **2002**, *124*, 7660-7661.

(43) Jantunen, K. C.; Burns, C. J.; Castro-Rodriguez, I.; Da Re, R. E.; Golden, J. T.; Morris, D. E.; Scott, B. L.; Taw, F. L.; Kiplinger, J. L. *Organometallics* **2004**, *23*, 4682-4692.

(44) Kiplinger, J. L.; Morris, D. E.; Scott, B. L.; Burns, C. J. *Organometallics* **2002**, *21*, 3073-3075.

(45) Schelter, E. J.; Veauthier, J. M.; Thompson, J. D.; Scott, B. L.; John, K. D.; Morris, D. E.; Kiplinger, J. L. *J. Am. Chem. Soc.* **2006**, *128*, 2198-2199.

(46) Silva, M.; Antunes, M. A.; Dias, M.; Domingos, A.; dos Santos, I. C.; Marcalo, J.; Marques, N. *Dalton Trans.* **2005**, 3353-3358.

(47) Stewart, J. L.; Andersen, R. A. *New J. Chem.* **1995**, *19*, 587-595.

(48) Edelstein, N. M.; Lander, G. H. Magnetic Properties. In *The Chemistry of the Actinide and Transactinide Elements*, 3rd ed.; Morss, L. R., Edelstein, N. M., Fuger, J., Eds.; Springer: The Netherlands, 2006; Vol. 4, pp 2241-2247.

(49) Arnold, P. L.; Patel, D.; Wilson, C.; Love, J. B. *Nature* **2008**, *415*, 315-318.

(50) Miyake, C.; Hirose, M.; Ohya-Nishiguchi, H. *Inorg. Chim. Acta* **1989**, *165*, 179-183.

(51) Selbin, J.; Ahmad, N.; Pribble, M. J. *J. Chem. Soc., Chem. Commun.* **1969**, 759-760.

(52) Selbin, J.; Ahmad, N.; Pribble, M. J. *J. Inorg. Nucl. Chem.* **1970**, *32*, 3249-3258.

(53) A ^{1}H NMR of **14** was not observed across the temperature range 0-100 °C.

(54) This trend in chemical shift for like protons as a function of halide has been seen for other paramagnetic uranium systems: (a) $[(1,3\text{-}R_2\text{-}C_5H_3)_2UX]_2$ (R = $SiMe_3$, CMe_3; X = F, Cl, Br, I): Lukens Jr., W. W.; Beshouri, S. M.; Stuart, A. L.; Andersen, R. A. *Organometallics* **1999**, *18*, 1247-1252. (b) $(C_5Me_5)_3UX$ (X = F, Cl, Br): Evans, W. J.; Nyce, G. W.; Johnston, M. A.; Ziller, J. W. *J. Am. Chem. Soc.* **2000**, *122*, 12019-12020. (c) $(1,3\text{-}R_2\text{-}C_5H_3)_2UX_2$ (R = $SiMe_3$, CMe_3; X = F, Cl, Br, I): Lukens Jr., W. W.; Beshouri, S. M.; Blosch, L. L.; Stuart, A. L.; Andersen, R. A. *Organometallics* **1999**, *18*, 1235-1246. The ^{1}H NMR behavior of the $(C_5H_5)_3UX$ system has also been extensively studied not only where X = halide, but also for other donor groups such as OR, NR_2, SR, PR_2, etc.: Fisher, R. D. NMR-Spectroscopy of organo-f-element and pre-lanthanoid complexes. In *Fundamental and Technological Aspects of Organo-f-Element Chemistry*. Marks, T. J.; Fragala, I. L., Eds.; NATO ASI Series - Series C: Mathematical and Physical Sciences. D. Reidel Publishing Company: Dordrecht, 1985; Vol. 155, p 294.

(55) Dhingra, M. M.; Ganguli, P.; Mitra, S. *Chem. Phys. Lett.* **1974**, *25*, 579-581.

(56) Drago, R. S.; Wayland, B. B. *Inorg. Chem.* **1968**, *7*, 628-630.

(57) LaMar, G. N.; Fischer, R. H.; Horrocks, W. D., Jr. *Inorg. Chem.* **1967**, *6*, 1798-1803.

(58) While positive-feedback IR compensation was employed in the collection of the voltammetric data, there is still some contribution from uncompensated solution resistance to the potential separation between cathodic and anodic peaks. Thus, deviations in the peak separation from 60 mV cannot be attributed solely to heterogeneous electron-transfer kinetic effects.

(59) Lichtenberger, D. L.; Renshaw, S. K.; Bullock, R. M. *J. Am. Chem. Soc.* **1993**, *115*, 3276-3285.

(60) Wong, C.-Y.; Che, C.-M.; Chan, M. C. W.; Han, J.; Leung, K.-H.; Phillips, D. L.; Wong, K.-Y.; Zhu, N. *J. Am. Chem. Soc.* **2005**, *127*, 13997-14007.

(61) Lever, A. B. P. *Inorganic Electronic Spectroscopy*, 2nd ed.; Elsevier: Amsterdam, The Netherlands, 1984.

(62) (a) BrukerAXS, *SAINT 7.06*, Integration Software; Bruker Analytical X-ray Systems: Madison, WI, 2003. (b) Sheldrick, G. M. *SADABS 2.03*, Program for Adsorption Correction; University of Göttingen: Göttingen, Germany, 2001. (c) Sheldrick, G. M. *SHELXTL 5.10*, Structure Solution and Refinement Package; Universitiy of Göttingen: Göttingen, Germany, 1997.

(63) Tobia, D.; Baranski, J.; Rickborn, B. *J. Org. Chem.* **1989**, *54*, 4253-4256.

(64) Waggoner, K. M.; Power, P. P. *Organometallics* **1992**, *11*, 3209-3214.

(65) Barriere, F.; Geiger, W. E. *J. Am. Chem. Soc.* **2006**, *128*, 3980-3989.

(66) Barnhart, D. M.; Clark, D. L.; Grumbine, S. K.; Watkin, J. G. *Inorg. Chem.* **1995**, *34*, 1695-1699.

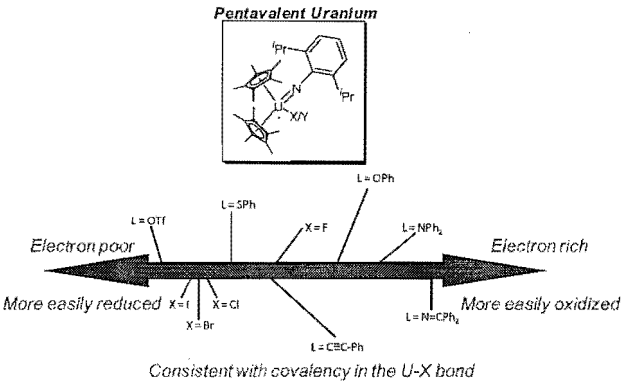
Pentavalent Uranium
L = OPh
L = SPh
L = OTf
X = F
L = NPh2
Electron poor
Electron rich
More easily reduced
X = I
X = Cl
X = Br
L = N=CPh2
More easily oxidized
L = C≡C-Ph
Consistent with covalency in the U-X bond